MOLECULAR AND CELLULAR BIOLOGY, Nov. 2008, p. 6903–6918 Vol. 28, No. 22
0270-7306/08/$08.00+0 doi:10.1128/MCB.01210-08

Sir3-Nucleosome Interactions in Spreading of Silent Chromatin in *Saccharomyces cerevisiae*▽

Johannes R. Buchberger,[1,2] Megumi Onishi,[1,2] Geng Li,[1,2] Jan Seebacher,[1] Adam D. Rudner,[1]§ Steven P. Gygi,[1] and Danesh Moazed[1,2]*

Howard Hughes Medical Institute[2] and Department of Cell Biology, Harvard Medical School,[1] 240 Longwood Ave., Boston, Massachusetts 02115

Received 31 July 2008/Returned for modification 22 August 2008/Accepted 8 September 2008

Silent chromatin in *Saccharomyces cerevisiae* is established in a stepwise process involving the SIR complex, comprised of the histone deacetylase Sir2 and the structural components Sir3 and Sir4. The Sir3 protein, which is the primary histone-binding component of the SIR complex, forms oligomers in vitro and has been proposed to mediate the spreading of the SIR complex along the chromatin fiber. In order to analyze the role of Sir3 in the spreading of the SIR complex, we performed a targeted genetic screen for alleles of *SIR3* that dominantly disrupt silencing. Most mutations mapped to a single surface in the conserved N-terminal BAH domain, while one, L738P, localized to the AAA ATPase-like domain within the C-terminal half of Sir3. The BAH point mutants, but not the L738P mutant, disrupted the interaction between Sir3 and nucleosomes. In contrast, Sir3-L738P bound the N-terminal tail of histone H4 more strongly than wild-type Sir3, indicating that misregulation of the Sir3 C-terminal histone-binding activity also disrupted spreading. Our results underscore the importance of proper interactions between Sir3 and the nucleosome in silent chromatin assembly. We propose a model for the spreading of the SIR complex along the chromatin fiber through the two distinct histone-binding domains in Sir3.

Saccharomyces cerevisiae silent chromatin is functionally analogous to heterochromatin in higher eukaryotes and is involved in stable gene repression and the maintenance of genomic stability. Silent chromatin is inherited epigenetically and is generally characterized by low levels of transcription, inhibition of DNA recombination, and late replication origin firing (11, 30, 36, 40). In *S. cerevisiae*, silencing occurs in three genomic regions: the silent mating type cassettes *HML* and *HMR*, telomeres, and ribosomal DNA repeats (40). The mating type cassettes and telomeres require the SIR complex, consisting of the histone deacetylase Sir2 and the structural components Sir3 and Sir4.

Like heterochromatin in higher eukaryotes, silent chromatin is distinguished from euchromatin by particular posttranslational modification states of its nucleosomes, most notably the absence of lysine acetylation on the N-terminal tails of histones H3 and H4 (47). Sir2 is an NAD-dependent histone deacetylase and is the major deacetylase involved in silent chromatin assembly (19, 24, 43). Sir2-mediated deacetylation is a required step in the formation of silent chromatin (16, 28, 39); the SIR complex has higher affinity for deacetylated histone tails and is therefore able to bind to nucleosomes that have been deacetylated by Sir2 (13, 27, 34). Furthermore, Sir2 releases the metabolite *O*-acetyl-ADP-ribose (AAR) during deacetylation (20, 48, 50), which triggers a conformational change in the SIR complex (27) and is required for the formation of SIR-nucleosome filaments (34) in vitro.

The establishment phase of silent chromatin can be conceptualized as a nucleation step at the silencer site, followed by a subsequent spreading phase along the chromatin fiber (16, 28, 30, 39). During nucleation, Sir2, Sir3, and Sir4 are recruited to chromatin, leading to the deacetylation of histone H4. As a result, Sir3 can bind to the N-terminal tail of H4, an interaction that stabilizes the seeding complex and sets the stage for spreading. SIR proteins interact extensively with each other, leading to the recruitment of further SIR complex components to chromatin. Subsequent cycles of Sir2-Sir4 recruitment and histone deacetylation are proposed to mediate the spreading of the SIR complex along the chromatin fiber.

Sir3 binds to multiple factors that are involved in silent chromatin formation, most notably to itself through dimerization, as well as Sir4, histones H3 and H4, and Rap1, a DNA-binding protein that recruits the SIR complex to chromatin (13, 23, 26, 31, 32). Sir3 contains two conserved domains. The N-terminal 214 residues of Sir3 form a bromo-adjacent homology (BAH) domain (53), which has recently been shown to bind to nucleosomes (34). Furthermore, within its C-terminal half lies an AAA$^+$ (*A*TPases *a*ssociated with a variety of cellular *a*ctivities) domain (33, 44), which has no detectable ATPase activity but overlaps with two patches that interact with histone tails in vitro, residues 623 to 762 and 799 to 910 (13). It is still unclear how these three histone-binding activities are coordinated to function within silent chromatin. However, consistent with the body of data highlighting the particular importance of histone 4 lysine 16 (H4K16) for silencing in vivo, Sir3-histone binding has been

* Corresponding author. Mailing address: Department of Cell Biology, Harvard Medical School, 240 Longwood Ave., Boston, MA 02115. Phone: (617) 432-1258. Fax: (617) 432-1144. E-mail: danesh@hms.harvard.edu.

§ Present address: Ottawa Institute of Systems Biology, Department of Biochemistry, Microbiology, and Immunology, University of Ottawa, 451 Smyth Rd., Ottawa, Ontario KlH 8M5, Canada.

▽ Published ahead of print on 15 September 2008.

TABLE 1. Yeast strains used in this study

Strain	Relevant genotype[a]	Reference or source
W303a	*MAT***a** *ade2-1 can1-100 his3-11 leu2-3,112 trp1 ura3-1 GAL*	J. Rine
SF10 (BJ5459)	*MAT***a** *ura3-52 trp1 lys2-801 leu2Δ1 his3Δ200 pep4Δ::HIS$_3$ prb1Δ1.6R can1*	E. Jones
ADR3081	*MAT***a** *his1-1*	This study
ADR3107	W303a *hmlΔ::TRP1 SIR3-MYC$_{13}$::KAN^R sir4Δ::Nat^R*	This study
DMY296 (UCC3505)	*MAT***a** *ade2-101 his$_3$-Δ200 leu2-Δ1 lys2-801 trp1-63 ura3-52 ppr1::HIS$_3$ adh4::URA3-TEL-VIIL ADE2-TELVR*	42
DMY3314	W303a *hmrΔE::TRP1 TELVII-L::URA3*	This study
DMY3315	DMY3314 *sir3Δ::Kan^R*	This study
DMY3628	W303a *pep4Δ::LEU2 SIR3-TAP-*Kl*TRP1*	34
DMY3727	DMY3314 *sir2Δ::Nat^R*	This study
DMY3863	W303a *pep4Δ::LEU2 SIR3*(Δ*BAH*)*-TAP-*Kl*TRP1*	34
DMY3875	SF10 *sir3Δ::Kan^R*	This study
DMY4071	W303a *pep4Δ::LEU2 SIR3*(*D17G*)*-TAP-*Kl*TRP1*	This study
DMY4072	W303a *pep4Δ::LEU2 SIR3*(*E84K*)*-TAP-*Kl*TRP1*	This study
DMY4073	W303a *pep4Δ::LEU2 SIR3*(*K202E*)*-TAP-*Kl*TRP1*	This study
DMY4074	W303a *pep4Δ::LEU2 SIR3*(*L738P*)*-TAP-*Kl*TRP1*	This study
DMY4085	W303a *pep4Δ::LEU2 SIR3*(Δ*BAH*)*-MYC$_{13}$-Kan^R*	This study
DMY4086	W303a *pep4Δ::LEU2 SIR3*(Δ*BAH*/*L738P*)*-MYC$_{13}$-Kan^R*	This study
DMY4090	W303a *pep4Δ::LEU2 SIR3*(*S67P*)*-TAP-*Kl*TRP1*	This study
DMY4091	W303a *pep4Δ::LEU2 SIR3*(*E95K*)*-TAP-*Kl*TRP1*	This study
DMY4092	W303a *pep4Δ::LEU2 SIR3*(*E137K*)*-TAP-*Kl*TRP1*	This study
DMY4093	W303a *pep4Δ::LEU2 SIR3*(*P179L*)*-TAP-*Kl*TRP1*	This study
DMY4094	W303a *pep4Δ::LEU2 SIR3*(*S212F*)*-TAP-*Kl*TRP1*	This study

[a] Kl*TRP1*, *Kluyveromyces lactis TRP1* gene.

shown to be sensitive to H4K16 acetylation both in BAH and the C-terminal histone-binding (CHB) region (27, 34).

Sir3 binds to chromatin during the initial recruitment step but is also required for the spreading of silent chromatin, since none of the other components are able to spread in its absence (16, 39). Indeed, it is the limiting component in spreading, as increasing its dosage results in silent subtelomeric domains that extend far beyond what is seen with endogenous levels of Sir3, to more than 20 kb from the end of the chromosome (14, 35).

In order to examine which activities of Sir3 are required for downstream spreading rather than initial recruitment, we performed a directed screen for dominant *SIR3* mutations that disrupt silencing in a *SIR*$^+$ strain. This class of alleles is predicted to produce proteins that poison the spreading of silent chromatin during the establishment process. We found that the BAH domain is especially sensitive for mutations in this type of screen, as 21 out of a total of 22 mutants were recovered within this domain. L738P is the only mutant residue found outside of BAH, lying in the AAA$^+$ domain of Sir3 within one of the CHB patches. The BAH point mutants tested, but not Sir3-L738P, disrupt the interaction of Sir3 with bulk nucleosomes, demonstrating the significance of the Sir3-nucleosome interaction for the spreading of silent chromatin. In contrast, L738P binds to the amino tail of H4 more strongly than wild-type Sir3 in vitro. The results presented here indicate that the spreading of silent chromatin relies on multiple coordinated Sir3-histone interactions, with the BAH domain serving as the main anchor of Sir3 to chromatin.

MATERIALS AND METHODS

Plasmids and strains. The strains and plasmids used in this study are listed in Tables 1 and 2. To construct pDM832, the *SIR3* open reading frame (ORF) was mutagenized in pAR467 (*SIR3* in pRS315) by using site-directed mutagenesis to introduce silent mutations recognized by AatII (at residue +767) and MluI (at residue +2209) (54). A tag including the tobacco etch virus recognition site and three FLAG repeats, as well as the *ADH1* terminator, was subcloned into the resulting vector. This construct was used for the screen, and all mutants were expressed from a corresponding derivative vector.

Screen. Mutagenesis was carried out by using standard *Taq* polymerase-mediated PCR (30 cycles) to amplify four overlapping fragments from pDM832 with the following primer pairs: (i) ATAGTATGAAAAAGAAAACAC and CAGA AGGGGACGCCGATGAG, (ii) CGAACCTACTGCGGAAAAGT and CTTG TGATTTTAGTAGTTCT, (iii) TATGAACGAAAATCCTAC and ACGTTGG CTACGTTCTTTGC, and (iv) TCCGGAAAATCTATTGAG and GCTTATTT AGAAGTGGCGCG.

Three micrograms pDM832 was digested with BlpI/AatII, AatII/HindIII, HindIII/MluI, or MluI/NcoI and cotransformed with 10 μg of the corresponding PCR product into the *ADE2* reporter strain (DMY296) (42). Fivefold serial dilutions were plated and grown at 30°C for 2 days to determine the optimal colony number per plate (transformation mixes were stored at 4°C). The entire mix was subsequently plated onto synthetic complete medium without leucine (SC −Leu) (0.5 mg/liter Ade) to yield approximately 300 to 400 colonies per plate. The plates were incubated for 3 to 4 days at 30°. White colonies were restreaked onto the same medium to confirm color formation.

Secondary silencing screen and silencing assays. For positive hits, plasmids were extracted from yeast by bead beating in phenol-chloroform breaking buffer (2) and transformed into *E. coli* cells, miniprepped, and transformed into strain DMY3314 (*SIR3*$^+$) or DMY3315 (*sir3*Δ). Silencing assays were performed as described previously (34). Confirmed hits were sequenced using primer pairs (i) CAGACTCAATACACTTAA and ACTAGAAAATCTCTATCC, (ii) AAACA TCTGTGCTTTCAA and ATTTTACTGCTCAATTCG, (iii) CCCAAAATAA ACTATTTT and CTCAATAGATTTTCCGGA, and (iv) TGGTACCACGCT ATTTCT and AGGCACCGCATATGACCT.

Structural analysis. Structures were obtained from the protein databank (www.pdb.org). The Sir3-BAH monomer depicted in Fig. 1 and 10 represents PDB-ID 2FL7 (17), and the BAH dimer which is shown in Fig. 7C, represents PDB-ID 2FVU (6). The yeast nucleosome shown in Fig. 10 represents PDB-ID 1ID3 (52). All figures were prepared by using MacPyMOL software (DeLano Scientific, Palo Alto, CA; www.pymol.org).

Quantitative mating assay. A *MAT*α *his1-1* strain (38) was grown to an optical density at 600 nm (OD_{600}) of ~4.0 in yeast extract-peptone-dextrose (YEPD) medium and strains to be tested (DMY3314 or 3315 carrying the mutant constructs on a vector) to an OD_{600} of ~1.0 in SC −Leu medium. Three hundred microliters of the tester (*MAT*α *his1-1* strain) was mixed with 10-fold serial dilutions of the tested strain, ranging from 10^1 to 10^7 cells. The mating mix was plated onto minimal medium. Additionally, the two highest dilutions of the

TABLE 2. Plasmids

Plasmid	Description	Reference or source
pRS315	*CEN/ARS LEU2*	41
pRS316	*CEN/ARS URA3*	41
pRS425	2μm *LEU2*	5
pDM456	pGEX GST	13
pDM457	pGEX GST-H4(15–34)	13
pDM832	pRS315 Sir3(AatII/MluI)-TEV-FLAG	This study
pDM862[a]	D17G	This study
pDM863	T63A	This study
pDM865	S67P	This study
pDM866	E84K	This study
pDM867	W86G	This study
pDM868	W93R	This study
pDM870	E95K	This study
pDM871	L96F	This study
pDM873	A136V	This study
pDM875	E137G	This study
pDM876	E137K	This study
pDM877	P179L	This study
pDM879	A181T	This study
pDM880	V196I	This study
pDM881	P201L	This study
pDM882	K202E	This study
pDM885	S204P	This study
pDM887	K209N	This study
pDM888	K209R	This study
pDM889	S212F	This study
pDM890	K219E	This study
pDM892	L738P	This study
pDM1009	Gal1-10 Sir3-$FLAG_3$ in pRS425	This study
pDM1011	pDM1009 L738P	This study
pDM1002	pDM1009 D17G	This study
pDM1004	pDM1009 E84K	This study
pDM1007	pDM1009 K202E	This study
pDM1027	Sir3BAH-only wt in pRS315	This study
pDM1028	Sir3BAH-only D17G in pRS315	This study
pDM1029	Sir3BAH-only E95K in pRS315	This study
pDM1030	Sir3BAH-only E202K in pRS315	This study
pDM1104	Sir3BAH-FLAG in pRS316	This study
pDM1105	Sir3-BAHΔ derivative of pDM832	This study
pDM1138	pDM457 K16Q	This study
pDM1139	pDM457 K16R	This study
pDM1164	pDM1009 L738P	This study
pDM1165	pDM1009 BAHΔ-L738P	This study
pDM1166	pDM832 K99E	This study
pDM1167	pDM832 E84K/K99E	This study

[a] Plasmids pDM862 to pDM892 are mutant derivatives of pDM832.

tested strain were plated onto SC −Leu medium to count total colony numbers. The mating efficiency was calculated as the ratio of the number of diploid colonies on minimal medium divided by the number of haploid colonies on SC −Leu medium. For each experiment, the average of the results from three plates was calculated. The assays were repeated two to three times.

ChIP. Chromatin immunoprecipitation (ChIP) assays were performed as described previously (38), with the following modifications: for FLAG ChIP, 5 μl anti-FLAG M2-agarose beads (Sigma) were added to lysates. For total Sir3 ChIP, 0.5 μl polyclonal anti-Sir3 antibody and 5 μl magnetic protein A beads (Dynal) were added to lysates. Lysates were incubated at 4°C for 2 h with end-over-end rotation. After elution, 200 μl TE50/10 (50 mM Tris-HCl, 10 mM EDTA) with 1% sodium dodecyl sulfate was added to the reserved lysate for input samples. One hundred micrograms proteinase K was added in 250 μl TE, and samples were incubated overnight at 65°C to reverse cross-links and digest total protein. All samples were phenol-choloroform extracted once, chloroform extracted once, and precipitated by adding 20 μg glycogen, 45 μl 0.3 M NaOH, and 1 ml cold ethanol. Samples were centrifuged for 10 min at 14,000 rpm, the pellets were washed once in 70% ethanol and centrifuged again, and the new pellets were air dried. Pellets were resuspended in 50 μl TE10/1 with 10 μg RNase A and incubated at room temperature for 1 h. PCRs were carried out as described below, with the following primer pairs (18, 28): TEL0.07, CAT GACCAGTCCTCATTTCCATC and ACGTTTAGCTGAGTTTAACG GTG; TEL0.7, TGAGTTTAACGGTGGCATAT and GGACAGATCCTTT CGCATTCCTAC; TEL2.4, CTGGATGATAAATGGACCTGTCCTTC and GGCGAGCTGAATCCCGAACTTTGT; and *ACT1*, GCCTTCTACGTTTC CATCCA and GGCCAAATCGATTCTCAAAA.

PCR amplifications were carried out with 27 to 30 cycles, depending on the linear range of each sample. Samples were run on 6% polyacrylamide gel electrophoresis (PAGE) gels in 1× TBE (Tris-borate-EDTA). Quantification was performed by using Phosphoimager analysis and QuantityOne software (Bio-Rad).

Coimmunoprecipitation. All coimmunoprecipitation assays were performed as described previously (34). Strain DMY3315 with the corresponding Sir3-FLAG *CEN* plasmid was used for Sir2-Sir4 IPs. Strains ADR3107, DMY4085, and DMY4086 transformed with the corresponding *CEN* plasmids were used for Sir3-Sir3 IPs. For FLAG IPs, 5 μl anti-FLAG M2-agarose (Sigma) was added and bound for 1 h. Western blots were performed with anti-FLAG M2-horseradish peroxidase antibody (1:5,000; Sigma) or polyclonal Sir2 or Sir4 antibody (1:5,000) (49), followed by anti-rabbit horseradish peroxidase-linked secondary antibody (1:10,000).

FLAG purification. Purifications were done as described previously (4) with the following modifications. DMY3875 carrying Sir3-3xFLAG on *CEN* or pGal-2μm plasmids was grown in liquid SC −Leu medium to an OD_{600} of ~2.0, harvested, and frozen in liquid N_2 (for Gal inductions, cells were grown overnight in 2% raffinose and induced for 9 h with 2% galactose). Four to 5 g of frozen cells was thawed in an equal volume of lysis buffer (150 mM NaCl, 50 mM HEPES, pH 7.5, 10 mM magnesium acetate, 1 mM EDTA, 50 mM β-glycerophosphate, 0.5% NP-40, 5% glycerol, 0.5 mM dithiothreitol, 1 mM phenylmethylsulfonyl fluoride), bead beaten in multiple 2-ml tubes twice for 30 s, and collected. Lysates were centrifuged at 14,000 rpm in chilled microcentrifuges for 10 min, and supernatant was pooled and bound for 2 h to 100 μl (*CEN* plasmids) or 200 μl (pGal-2μm plasmids) anti-FLAG M2-agarose (Sigma). Beads were washed in batch mode twice for 5 min, once for 10 min with lysis buffer, and once for 10 min in hemagglutinin buffer (100 mM HEPES, pH 7.5, 100 mM sodium acetate, 1 mg/ml hemagglutinin dipeptide) and were eluted at room temperature with an equal volume of elution buffer (100 mM HEPES, pH 7.5, 150 mM sodium acetate, 200 μg/ml $FLAG_3$ peptide).

MS. One quarter of the elution was precipitated with trichloroacetic acid and analyzed as described previously (4), with slight modifications. Peptides were separated across a 45-min gradient ranging from 7% to 30% (vol/vol) acetonitrile in 0.1% (vol/vol) formic acid in a microcapillary (125 mm by 18 cm) column packed with C_{18} reverse-phase material (Magic C18AQ with 5-μm particles and 200-Å pore size; Michrom Bioresources) and on-line analyzed on a hybrid linear ion trap Orbitrap mass spectrometer (LTQ Orbitrap; Thermo-Electron). The tandem mass spectrometry (MS-MS) spectra were searched by using the Sequest algorithm. Peptide matches were filtered to 1% false positives by using a target-decoy database strategy. Proteins identified in an untagged mock purification were subtracted from the total list of tagged purifications.

Native PAGE. Three micrograms purified protein was loaded onto 3-to-12% blue native gels (NativePAGE Novex; Invitrogen) in a total volume of 10 μl. Samples were run for 60 min at 150 V and 50 min at 250 V at 4°C. Gels were fixed and destained overnight in 50% methanol, incubated for 10 min in 5% methanol, and subsequently silver stained.

Histone tail binding. Plasmids expressing glutathione *S*-transferase (GST) and GST fused to residues 15 to 34 of the H4 amino terminus [GST-H4(15-34)] (13) were grown in *E. coli* BL21(DE3) cells. The K16Q (pDM1137) and K16R (pDM1138) constructs were made from pDM457 by site-directed mutagenesis (54). Cultures (720 ml) were inoculated with 80 ml overnight culture in the presence of 1 mM isopropyl-β-D-thiogalactopyranoside (IPTG), incubated on a shaker for 2 h at 37°C, and harvested. Pellets were resuspended in 16 ml lysis buffer (20 mM Tris, pH 8.0, 150 mM NaCl, 1 mM EDTA, 1% Triton X-100, 1 mM dithiothreitol, 1 mM phenylmethylsulfonyl fluoride), sonicated 10 times for 30 s in a Branson Sonifier 450 (40% amplitude), and bound to 1 ml glutathione agarose (Sigma) for 1 h at 4°C. Beads were washed three times in wash buffer (same as lysis buffer with 0.1% Triton X-100) and stored in an equal volume of buffer at 4°C in the presence of 0.02% NaN_3. Three micrograms of purified Sir3 was incubated with 7 μg GST or GST fusion protein for 1 h in binding buffer at 4°C, as described previously (13). Beads were washed three times in binding

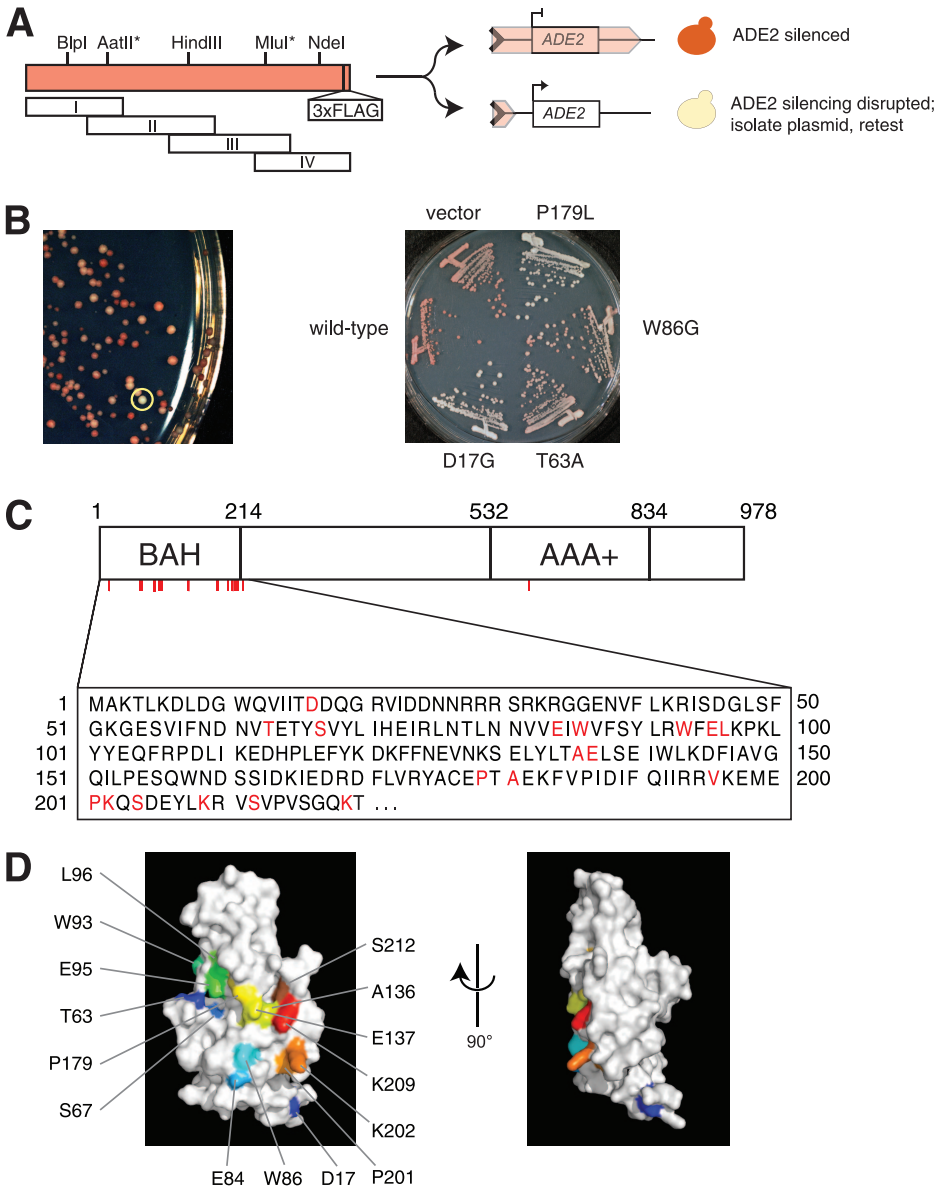

FIG. 1. Isolation of dominant negative *SIR3* alleles. (A) Two silent mutations were introduced into the *SIR3* ORF (denoted by asterisks) to allow excision of specific fragments. The resulting *SIR3*-containing plasmid was digested with two adjacent restriction endonucleases (shown above the Sir3 diagram) and cotransformed with the corresponding PCR fragment (I to IV) into a *TELVR*::*ADE2* reporter strain. Red or red/white sectored colonies are indicative of wild-type silencing, while white colonies indicate loss of silencing. These white transformants were isolated as positive hits. (B) Sample plate with a positive hit circled (left) and sample restreaks (right). (C) Locations of Sir3 mutations, with the primary sequence of the BAH domain shown in the box below. Mutations are indicated by red tick marks and red letters. L738P is the single mutation in the AAA+ domain. (D) Locations of the mutated residues in the BAH domain mapped onto the structure of the domain (PDB-ID 2FL7; see reference16). Ala181, Val196, and Ser204 are not shown as they lie internally in the structure. Lys219 and Leu738 are not part of the structure.

buffer, 20 μl sample buffer was added, and samples were run on a 10% (Sir3) or 15% (GST) PAGE gel (1/25 of the sample was loaded for GST and the rest for Sir3). For GST, gels were Coomassie stained, and immunoblots were performed for the FLAG tag to detect Sir3.

RESULTS

Genetic screen and resulting mutations. In order to identify *SIR3* alleles that dominantly disrupted silencing, we used a reporter strain that carried the *ADE2* reporter gene proximal to telomere *TELVR* (42) (Fig. 1A). In this strain, the *ADE2* marker is metastably silenced in wild-type cells, resulting in red or red/white sectored colonies. White colonies are indicative of active *ADE2* transcription and, therefore, disruption of silencing. We constructed a *SIR3* plasmid that allowed the screening of four separate fragments by introducing unique restriction sites into the *SIR3* ORF that allowed the excision of fragments of equal size. The gapped plasmid was cotransformed into the reporter strain with a PCR fragment containing homology on either side of the gap to allow for in vivo gap repair. White colonies obtained after transformation were further analyzed

TABLE 3. List of dominant negative mutations

Amino acid residue change	Nucleotide change
D17G	A50G
T63A	A187G
S67P	T199C
E84K	G250A
W86G	T256G
W93R	T277C
E95K	G283A
L96F	C286T
A136V	C407T
E137G	A410G
E137K	G409A
P179L	C536T
A181T	G541A
V196I	G586A
P201L	C602T
K202E	A604G
S204P	T610C
K209N	A627C
K209R	A626G
S212F	C635T
K219E	A655G
L738P	T2213C

as potential positive hits (Fig. 1B). After colony purification, plasmid DNA was recovered from these cells and retransformed into *ADE2*::*TELVR* cells to confirm that the dominant negative phenotype was plasmid linked. Positive plasmids were transferred to *E. coli* cells, purified, and sequenced to identify any mutations.

In total, we found 22 unique mutations, nearly all of which were located within (or just adjacent to) the N-terminal BAH domain, while only a single mutation, L738P, was located within the C-terminal half (Table 3; Fig. 1C). When the mutant residues were mapped on the available structures of the BAH domain (6, 17), it was remarkable that all mutated residues mapped on the same side of the structure (Fig. 1D), with the exception of A181T, V196I, and S204P, which were buried within the structure. This clustering suggests that the silencing defects observed in the BAH mutants are caused by a similar mechanism.

Strength of silencing defects. To further test for plasmid linkage of the phenotype and for independence from the *TELVR*::*ADE2* silencing reporter, all clones were tested in a second reporter strain carrying *TRP1* at the *HMR* silent mating type locus (*hmrΔe*::*TRP1*) with a weakened silencer (to increase sensitivity) and *URA3* at *TELVIIL* (*TELVIIL*::*URA3*) (Fig. 2). In these cells, the loss of TRP1 silencing at the HMR locus results in increased growth on medium lacking tryptophan (SC −Trp), and the loss of telomeric URA3 silencing results in loss of growth on medium containing 5-fluoroorotic acid, which is toxic to Ura^+ cells (10). The mutants disrupted silencing to various degrees, with most BAH mutations completely disrupting silencing at both reporters (Fig. 2). Some mutants had a partial defect, most notably the Sir3-V196I mutant (Fig. 2, row 17). As mentioned above, Val196 is not exposed to the surface in the BAH structure, and valine to isoleucine is a conservative substitution, providing a possible explanation for the weaker phenotype. The only non-BAH mutant, Sir3-L738P, caused only a minor disruption of *URA3* silencing but a complete loss of silencing of *TRP1* (Fig. 2, row 25).

Based on the results of sequence alignments, Leu738 is conserved among closely related budding yeast species and might therefore be sensitive to other substitutions. To determine whether the mutant phenotype was specific to the substitution of proline, we mutated Leu738 to alanine by site-directed mutagenesis. The Sir3-L738A mutant had no dominant silencing defect (Fig. 2, row 26), indicating that the disruption of silencing was residue specific at this location.

We also tested whether any of the mutants were able to rescue silencing in the absence of wild-type Sir3, using a *sir3*Δ derivative of the *hmrΔe*::*TRP1 TELVIIL*::*URA3* double-tester strain. As shown in Fig. 3, none of the mutants was able to rescue silencing at either locus, indicating that the dominant negative silencing defect was not due to the presence of a mixed population of mutant and wild-type Sir3 molecules; rather, these mutants exhibited a loss-of-silencing phenotype on their own. Sir3-L738A was able to partially rescue silencing, and thus has a much weaker loss-of-silencing defect than Sir3-L738P (Fig. 3, compare row 24 with row 25). However, the weak loss-of silencing defect observed with an alanine substitution demonstrates that this position is sensitive to substitutions other than proline.

Silencing defects with Sir3-BAHΔ and BAH only. Sir3 constructs lacking the BAH domain are unable to rescue silencing in a *sir3*Δ background, demonstrating that this domain is required for silencing (3, 34). Since most of the mutations lie within the BAH domain, we were interested in examining whether deleting the entire BAH domain also had a dominant defect, which would indicate that the point mutants act as a loss of function of this domain.

As shown in Fig. 4A (rows 1 and 2), the expression of Sir3-BAHΔ dominantly disrupted silencing at both loci tested, to the same extent as the expression of the strongest BAH alleles. This result was consistent with a report that the C-terminal fragment of Sir3 (residues 508 to 978) dominantly disrupts silencing at the telomere (9), which may be due to the absence of its BAH domain. Conversely, we also tested whether select BAH mutant domains expressing truncated proteins (residues 1 to 214 only) were dominant negative for silencing. Even though these constructs were expressed well (Fig. 4B), none disrupted silencing in the presence of wild-type Sir3 (Fig. 4A, rows 3 to 6), consistent with the hypothesis that the introduction of these mutations rendered the BAH domain nonfunctional and that the observed phenotype was not due to a gain of function of the BAH domain.

Dominant mating defects. In addition to the exogenous reporter genes, we were interested in examining the dominant silencing defect at an endogenous silencer and transcript. To this end, we performed quantitative mating assays to measure the ability of strains to mate as a readout for *HM* silencing (12). Given that Sir3-BAHΔ behaved like the strong BAH mutants in the previous silencing assays (Fig. 2 and 4A), we selected the deletion as a representative for all mutations in this domain. Sir3-BAHΔ exhibited a weak dominant mating defect, with a 61% decrease in mating efficiency (Fig. 4C). This dominant defect is much weaker than that at the telomere or at *hmrΔe*::*TRP1* (Fig. 2), but this difference is consistent with the robustness of *HML*/*HMR* silencing in general (40). Sir3-L738P

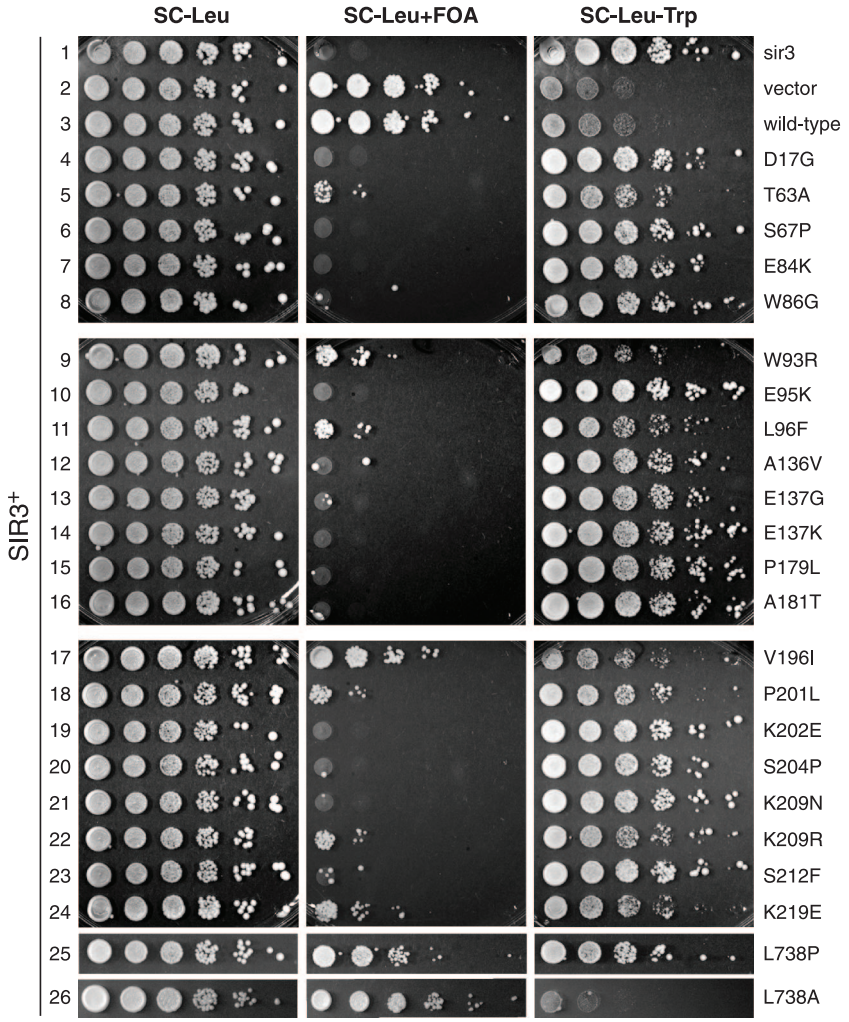

FIG. 2. Dominant negative silencing defects for telomeric URA3 and mating-type TRP1 (*TELVIIL*::*URA3 hmrΔe*::*TRP1*) reporters, respectively. The indicated Sir3 alleles are expressed from a *CEN* vector (pDM832 and its mutant derivatives). Growth on medium with 5-fluoroorotic acid (+FOA) and lack of growth on medium lacking tryptophan (−Trp) indicate silencing. Tenfold serial dilutions of wild-type and mutant strains were plated on the indicated growth medium. Most BAH mutants strongly disrupt silencing. L738P has a weaker defect (row 25). Replacing Leu738 with alanine does not disrupt silencing (row 26).

does not have a dominant negative mating defect at *HML*, consistent with it being a weaker allele.

Furthermore, we tested whether the BAHΔ and L738P mutants could rescue the mating defect of *sir3*Δ cells. As previously reported (3), in the absence of full-length Sir3, the BAHΔ mutant did not establish silencing at *HML* (Fig. 4D). Sir3-L738P, on the other hand, was able to partially rescue silencing, with only a 50-fold mating defect compared to the mating of wild-type Sir3. This defect was relatively weak and was in contrast to the results of the silencing assays using the TRP1 reporter at the *HMR* locus containing a weakened silencer (*hmrΔe*::*TRP1*), in which the Sir3-L738P mutant displayed a complete loss of silencing.

Mutant Sir3 proteins bind chromatin and decrease binding of total Sir3. Dominant negative mutations could disrupt silencing by a variety of mechanisms: mutants might interfere with the initial nucleation step or could act downstream during the spreading phase. To distinguish between these possibilities, we performed a series of ChIP assays. We first addressed whether the mutant proteins themselves were recruited to chromatin by analyzing the association of a subset of mutants with chromatin in the presence of wild-type *SIR3*. We selected representatives of BAH mutants such that each cluster of mutations in the structure was represented by one member (Fig. 1D). In addition, L738P was selected as the only non-BAH point mutation found. Chromatin was immunoprecipitated via the FLAG tag, which is specific to the plasmid-carried copy of *SIR3*. Sir3 binding was measured at *TELVIR*, which efficiently recruits the SIR complex (14). In this assay, all mutant Sir3 proteins were enriched at the telomere to levels intermediate between those of a *sir3*Δ control and wild-type Sir3 (Fig. 5A), indicating that the mutant Sir3 proteins were recruited to chromatin in the presence of wild-type Sir3.

To address the behavior of total Sir3, we used an anti-Sir3 antibody to measure Sir3 binding at increasing distances from the telomere in the same strain. In wild-type strains with en-

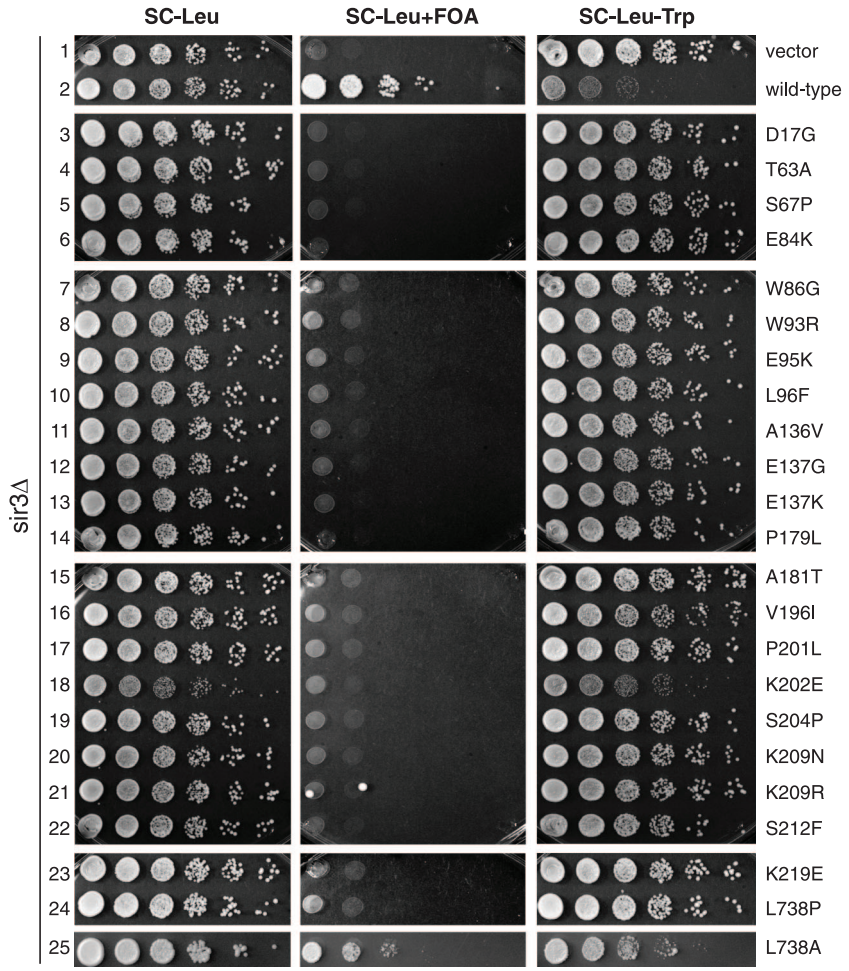

FIG. 3. Recessive silencing defects of Sir3 mutants. The indicated plasmids, producing wild-type or mutant Sir3, were introduced into *hmrΔe*::*TRP1 TELVIIL*::*URA3 sir3Δ*::*Kan*^{R} cells and assayed for silencing as described in the Fig. 2 legend. All mutants identified in the screen exhibit a complete loss of silencing (rows 3 to 24). The reduced growth in K202E (row 18) on SC −Leu −Trp medium is attributable to slower growth of this strain rather than partial rescue of silencing. L738A has a partial silencing defect (row 25). +FOA, with fluoroorotic acid; −Trp, without tryptophan.

dogenous *SIR3* levels, robust spreading of Sir3 has been observed up to a distance of 2.8 kb from the end of chromosome VIR (14, 16). However, in strains with a silencing defect, such as those with *SIR2* deleted, the only detectable binding of Sir3 occurs at the end of the chromosome; binding at more-distal sites is completely abolished in this situation (14, 16, 39). As shown in Fig. 5B, the introduction of any mutation reduced total Sir3 association with chromatin from 70 bp and 0.7 kb from the end of the chromosome. The observed spreading defect was less severe than the previously reported defect for a *sir2* deletion strain (16). However, it is likely that wild-type and dominant negative Sir3 proteins compete for binding, explaining the partial reduction, as opposed to a complete loss, of Sir3 binding at 0.7 kb from *TELVIR* (TEL0.7).

Spreading defect of dominant Sir3 mutants. To examine the recruitment and spreading behavior of the mutants in the absence of wild-type Sir3, we performed ChIP analysis of a subset of mutants when they were expressed as the only source of Sir3 in the cell. As the behavior of the mutants had been similar in previous assays, the number of mutations for this and subsequent analysis was further reduced to three BAH mutations (D17G, E84K, and K202E) and L738P. In the absence of wild-type Sir3, all mutants tested were recruited to the end of chromosome *VIR* but not to more-distal sites (Fig. 5C). The pattern of enrichment for mutant Sir3 mirrored that of wild-type Sir3 when *SIR2* is deleted, a mutation previously determined to interfere specifically with spreading, but not initiation (16, 39), suggesting that these dominant negative alleles of Sir3 affect silencing primarily by disrupting the spreading of the SIR complex along chromatin.

None of the mutations affect the integrity of the SIR complex. We were next interested in identifying the underlying biochemical defect of the mutant proteins. We first examined the behavior of the mutants within the context of the SIR complex. In this complex, the main Sir3-interacting factors are Sir3 itself and Sir4, but a weak interaction with Sir2 has also been reported (15, 27, 31).

Since the function of Sir3 in silencing is intimately tied to the other two components of the SIR complex, we first tested the association of mutant Sir3 proteins with Sir2 and Sir4 using

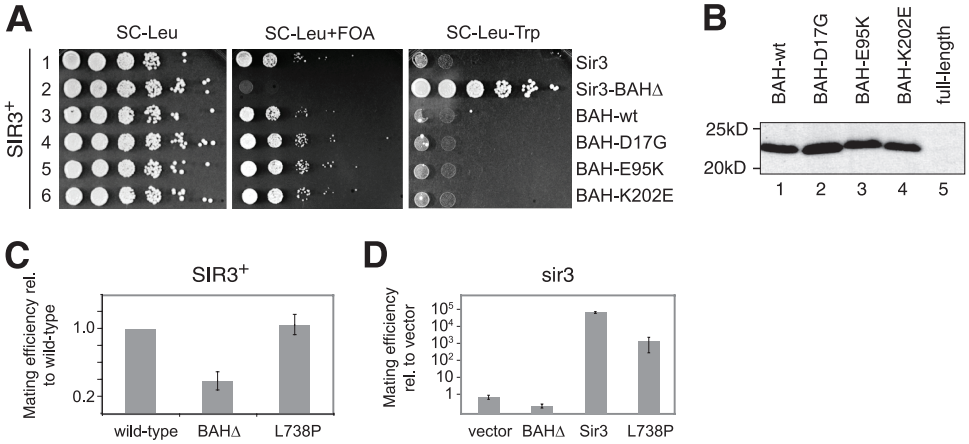

FIG. 4. Sir3 proteins lacking the BAH domain disrupt silencing in a dominant negative manner. (A) Sir3-BAHΔ dominantly disrupts silencing (row 2). Mutations expressed in the context of an isolated BAH domain (BAH only) do not disrupt silencing dominantly (rows 4 to 6). +FOA, with fluoroorotic acid; −Trp, without tryptophan. Silencing assays were performed as described in the Fig. 2 legend. (B) Western blot for expression of BAH only shows that the mutant BAH proteins are expressed at the same levels as wild-type BAH. Full-length Sir3-FLAG runs at ~120 kDa. (C) Dominant negative mating defects of Sir3-BAHΔ and Sir3-L738P at *HML*. BAHΔ mating efficiency is 0.39 ± 0.11 (mean ± standard deviation) ($n = 3$) relative to that of wild-type *SIR3*; L738P mutant has no dominant defect, with a relative efficiency of 1.05 ± 0.112 ($n = 2$). (D) Recessive mating defect at *HML* relative to efficiency of vector-only control. Wild-type Sir3 has a mating efficiency of $9.7 \times 10^4 \pm 1.2 \times 10^4$ (mean ± standard deviation) ($n = 3$). Sir3-BAHΔ does not rescue the mating defect of *sir3*Δ mutant (0.3 ± 0.08; $n = 3$). Sir3-L738P partially rescues the mating defect of *sir3*Δ mutant at $1.9 \times 10^3 \pm 1.5 \times 10^3$ ($n = 3$). wt, wild type; rel., relative.

coimmunoprecipitation assays. While minimal interaction with Sir4 has been mapped to residues 482 to 728 (23, 31), it remained possible that a conformational change introduced by L738P disrupts the interaction with Sir4 in this adjacent region. Furthermore, the BAH domain may have an unknown indirect effect on SIR complex assembly. We immunoprecipitated wild-type, D17G, E84K, K202E, and L738P Sir3-FLAG and blotted for Sir2 and Sir4. Sir2 and Sir4 both coimmunoprecipitated with mutant Sir3 to levels that were similar to that observed for wild-type Sir3 (Fig. 6A), indicating that the silencing defect observed with these mutations was not due to a disruption of the SIR complex.

In order to comprehensively examine the effects of mutations of Sir3 on its interactions with other proteins, we purified the selected mutants via the FLAG tag and analyzed the protein mixture by using liquid chromatography coupled to MS-MS. The main interacting factors identified for wild-type Sir3 were Sir4, Asf2, and Sir2 (Fig. 6B). The same factors copurified with all Sir3 mutant proteins analyzed, as well as with the Sir3-BAHΔ truncated protein. We obtained similar patterns for both a low-salt (150 mM) and a high-salt (500 mM) (data not shown) purification. The presence of Sir2 and Sir4 confirm that the SIR complex was intact in the Sir3 mutant cells. Asf2 (*a*nti-*s*ilencing *f*actor 2) is a poorly characterized protein that was originally identified by its silencing defect at the silent mating loci when overexpressed (25) and that physically associates with Sir3 (A. D. Rudner and D. Moazed, unpublished observations). Since we did not detect a difference in the association of Sir3 and Asf2 with the Sir3 mutants tested, we concluded that the dominant negative silencing defect of these Sir3 proteins was unrelated to their interaction with Asf2.

Sir3 self-association. To examine whether the mutations disrupted the interaction between wild-type and mutant Sir3, we introduced the subset of mutants into a strain expressing a wild-type Sir3-13xMyc fusion from its endogenous locus. To ensure that the Sir3-Sir3 interaction was not mediated through the SIR complex, a *sir4*Δ derivative was used. Sir4 forms dimers that interact with Sir3 and, in principle, such dimers may bridge wild-type and mutant Sir3 proteins. Neither the point mutations nor the BAH deletion disrupted the Sir3-Sir3 interaction, as assayed by coimmunoprecipitation (Fig. 7A). Furthermore, a double mutant with the BAH domain deleted and carrying the L738P substitution interacted normally with wild-type Sir3 (Fig. 7B), indicating that the BAH domain and the region disrupted by L738P did not redundantly contribute to Sir3 self-association. Based on these results, we concluded that Sir3 was able to dimerize in the presence of the above mutations, consistent with reports mapping the minimal domain for Sir3 dimerization to residues 843 to 978 (26), a region that is unaffected by the substitutions recovered in our screen.

The BAH domain does not appear to interact with itself. In addition to the structure of the BAH monomer, Connelly et al. reported an extended helical fiber with two self-interaction surfaces, one on the side corresponding to the surface containing our BAH mutations and the other on the reverse side of the domain (Fig. 1D) (6). Based on these structural predictions, one potential interaction that may be disrupted by the BAH mutations may be BAH self-association. If the extended BAH fiber indeed reflects in vivo oligomerization, the silencing defect seen with mutant residues may be due to disruption of this interaction, and hence, of BAH-mediated Sir3 oligomerization.

Certain residues are in close contact with residues on the adjacent monomer, forming predicted salt bridges in the crystal structure. One such pair is Glu84 and Lys99, whose side chains are separated by 2.9 Å (Fig. 7C). Since E84K causes loss of silencing, we hypothesized that mutating Lys99 to glutamate would restore silencing by reestablishing the presumed salt bridge. By extension, the single mutant Sir3-K99E should have a dominant silencing defect as well, as the mutation of this

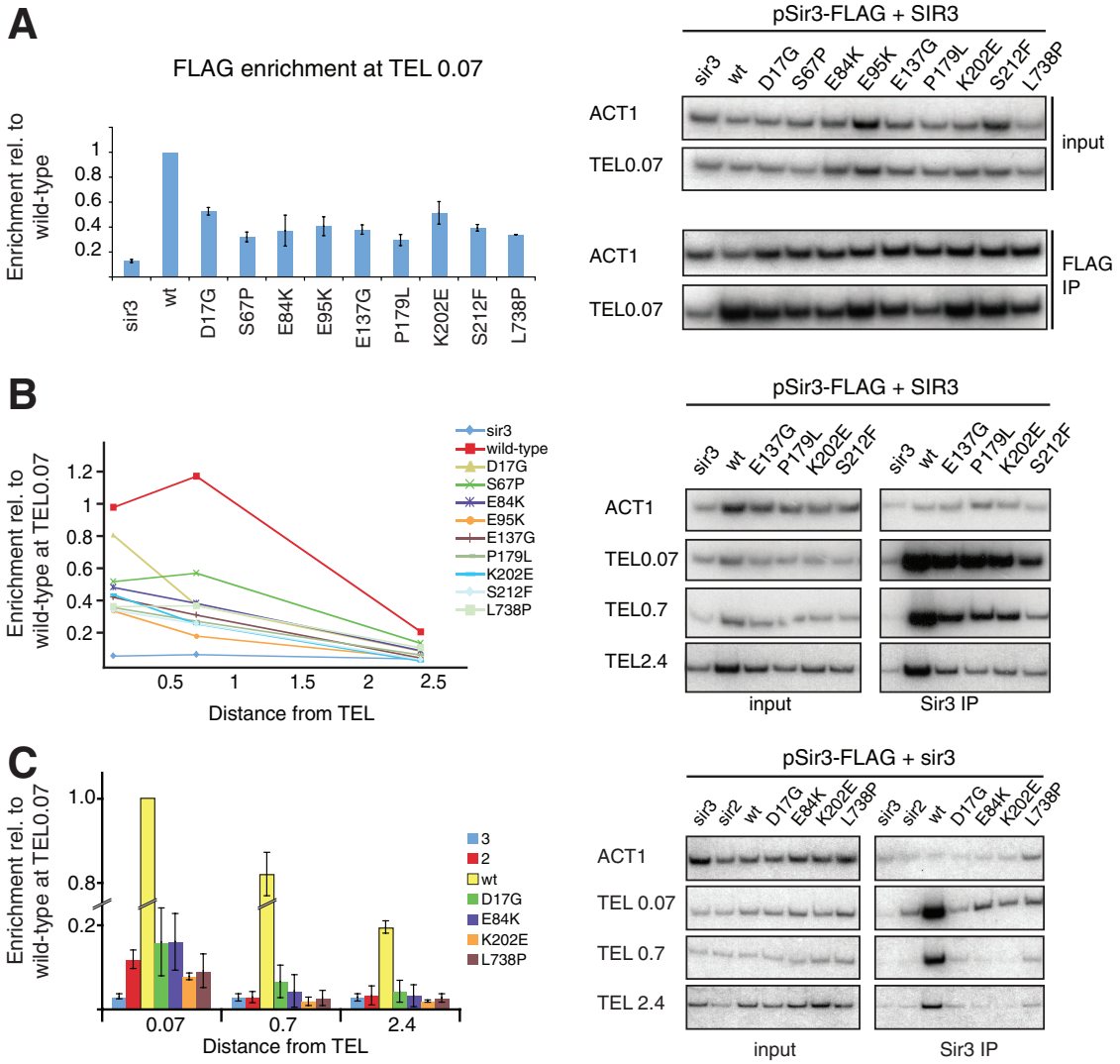

FIG. 5. Mutant Sir3 proteins are recruited to chromatin and interfere with total Sir3 spreading. (A) Dominant negative mutants are recruited to chromatin in cells that express wild-type *SIR3*. FLAG-tagged wild-type or mutant Sir3 was expressed from a *CEN* plasmid (pSir3) in a strain that also expressed endogenous *SIR3* (pSir3-FLAG + SIR3$^+$). The FLAG-tagged Sir3 was immunoprecipitated from lysates and the level of enrichment at *TELVIR* (TEL 0.07) was determined. *sir3*Δ represents a *sir3*Δ control strain with empty vector. Averages and standard errors are shown for the results of two experiments. (B) ChIP for total Sir3 in cells that express both wild-type *SIR3* and the indicated construct on a *CEN* plasmid (pSir3-FLAG + SIR3$^+$). *sir3*Δ is a control strain which had endogenous *SIR3* deleted and was transformed with empty vector. The level of enrichment was measured at 0.07, 0.7, and 2.4 kb from the end of chromosome VIR and is normalized to wild-type Sir3 at TEL0.07. Averages are shown for the results of three to five experiments, with the exception of E95K, for which are the averages of the results of two experiments are shown. (C) Sir3 point mutants are unable to spread along chromatin in the absence of wild-type Sir3. FLAG-tagged Sir3 was expressed from a *CEN* plasmid which was the only copy of *SIR3* (pSir3 + *sir3*Δ). *sir3*Δ (3Δ) carries an empty vector. *sir2*Δ (2Δ) has *SIR2* deleted but expresses endogenous *SIR3*. Averages and standard errors are shown for the results of two (TEL0.7, TEL2.4) or three (TEL0.07) experiments. wt, wild type; rel., relative.

residue from a positively to a negatively charged amino acid should disrupt this same interaction. We found, however, that the double mutant, Sir3-E84K/K99E, did not restore silencing in a *sir3*Δ strain, indicating that the second mutation did not function as an intragenic suppressor (Fig. 7D). Furthermore, in cells with *SIR3*, the double mutant still behaved as a dominant negative. Interestingly, the single mutant, Sir3-K99E, did not disrupt silencing and was able to fully rescue the silencing defect of *sir3*Δ cells (Fig. 7D). These results suggest that Glu84 and Lys99 are unlikely to interact as components of a salt bridge in vivo.

In addition to the structure-based genetic analysis, we tested for direct self-association of the BAH domain in coimmunoprecipitation assays. Using two differentially tagged BAH fusion proteins, we were unable to detect an interaction between two BAH domains or the BAH domain and full-length Sir3 in vivo (Fig. 7E, lanes 2 and 3), suggesting that this domain did not interact with itself. Furthermore, we were unable to detect an interaction between the BAH domain and a C-terminal fragment of Sir3 lacking the BAH domain (Fig. 7F), as would be expected if Sir3 would bind to itself in a head-to-tail orientation.

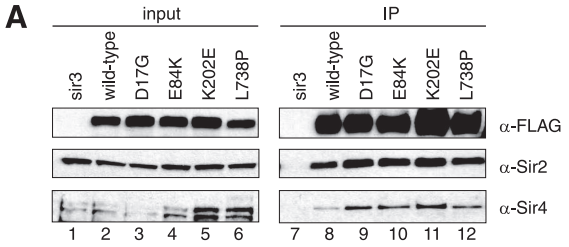

B

	wt			D17G			E84K		
	#	%	s.c.	#	%	s.c.	#	%	s.c.
Sir3	197	62.2	1.7	177	58.2	1.5	147	62.2	1.3
Sir4	48	36.5	0.31	46	34.7	0.30	28	22.5	0.18
Asf2	12	23.6	0.20	13	25.7	0.21	12	24.6	0.20
Sir2	8	16.2	0.13	9	19.8	0.14	8	17.8	0.13

	K202E			L738P			BAH		
	#	%	s.c.	#	%	s.c.	#	%	s.c.
Sir3	190	57.2	1.6	155	57.8	1.3	181	49.8	2.0
Sir4	45	33.8	0.30	28	20.8	0.18	42	35.6	0.28
Asf2	16	29.9	0.27	15	28.8	0.25	15	28.4	0.25
Sir2	11	30.2	0.17	4	7.8	0.06	11	28.3	0.17

FIG. 6. SIR complex formation is not disrupted by the Sir3 mutations. (A) Coimmunoprecipitation of the indicated Sir3 mutants with Sir2 and Sir4. (B) Liquid chromatography–MS-MS results for purified Sir3 proteins. The relative abundance of predominant binding partners is unchanged by point mutations or deletion of the BAH domain #, total number of peptides; %, percent coverage; s.c., spectral count; α, anti; wt, wild type.

In addition to forming dimers, Sir3 has been shown to oligomerize in vitro (27, 29). To directly test for oligomerization of the mutants, Sir3 proteins from overexpression constructs were purified from yeast, and the proteins were run on a native PAGE system that allowed the detection of higher-order assemblies. For wild-type Sir3, the bands detected were consistent with a distribution of mono-, di-, tri-, tetra- and hexamers, based on comparison with size standards (Fig. 7G, lane 1). The distribution of oligomers was unchanged for all mutant Sir3 proteins tested (lanes 2 to 5), indicating that none of the point mutants disrupted higher-order oligomer formation in this assay. Furthermore, we also analyzed the oligomerization behavior of Sir3-BAHΔ on native gels. While the deletion of the BAH domain resulted in a down-shift in the banding pattern, expected due to its smaller size, Sir3-BAHΔ still migrated in the gel as a ladder of bands consistent with distinct oligomeric species (Fig. 7G, lane 6). Therefore, the BAH domain was not required for oligomerization of Sir3 as detected by this assay. Furthermore, a double mutant (Sir3-BAHΔ/L738P) was also capable of forming oligomers (Fig. 7H, lane 2), excluding the possibility that the presence of the BAH domain masked a potential oligomerization defect of the L738P mutant.

BAH mutants disrupt the interaction of Sir3 with nucleosomes. Our laboratory has recently demonstrated a direct interaction between the BAH domain and nucleosomes (34). This interaction is disrupted in histone mutants that are known to disrupt silencing in vivo (K16Q and K16G); in *ard1*Δ cells, which abolish the N-terminal acetylation of Sir3; and in Sir3 truncation mutants that lack the BAH domain. Since Sir3-BAHΔ fails to interact with histones in this assay, we hypothesized that the dominant negative BAH point mutants may disrupt the same interaction. As shown in Fig. 8, compared to that of wild-type Sir3, the interaction between Sir3 proteins containing mutant BAH domains and histone H3 was diminished, while L738P did not affect this interaction. The binding defect was the weakest with the D17G mutant (Fig. 8A, 11th lane) but strong or complete with all other BAH mutants examined. Thus, the defects in nucleosome binding of the BAH domain mutants correlate well with the ability of these mutants to disrupt silencing in a dominant fashion.

L738P mutation increases the efficiency of Sir3-histone H4 tail interaction. The interaction between Sir3 and histones was originally described to occur between the N-terminal tails of histones H3 and H4 and the CHB regions of Sir3 in in vitro binding assays (13). Since the L738P mutation lies within one of the two tail-binding regions of Sir3, we were interested in whether this mutant affected binding to histone tails. In addition, in light of the results of the coimmunoprecipitation assays described above, BAH mutants may also disrupt binding to histone tails in this assay. We therefore examined these mutants in similar binding assays. Briefly, Sir3 purified from yeast was bound to GST fused to residues 15 to 34 of the H4 amino terminus (or GST only as a control) (Fig. 9A), as this patch on the N-terminal tail has been reported to interact with Sir3 in a manner that is sensitive to the identity of residue 16.

In this assay, neither the BAH point mutants nor the BAH deletion alters binding to GST-H4 in comparison to that of the wild type (Fig. 9B, lanes 1 to 4 and 6), indicating that the binding to this patch of histone H4 occurred independently of the BAH domain. In contrast, the L738P mutant displayed increased binding to GST-H4, both in the presence and absence of the BAH domain (Fig. 8B, lanes 5 and 7). Importantly, the observed increase did not reflect nonspecific binding, since the increased binding was lost when H4 carried the K16Q substitution (Fig. 9B), a mutation that has a silencing defect in vivo and loss of wild-type Sir3 binding in vitro (13, 22). The K16R substitution on H4 completely abolished the binding of wild-type Sir3 and Sir3-BAHΔ (Fig. 9C, lanes 9 to 12) but still bound to Sir3-L738P (Fig. 9C, lanes 13 to 16), indicating that H4K16R was more permissive to Sir3-L738P binding than to wild-type Sir3 binding.

DISCUSSION

Employing a screen for dominant negative alleles of *SIR3*, we identified a large collection of mutants whose expression disrupts telomeric and mating-type silencing. We found that all dominant negative mutants have a loss-of-silencing phenotype on their own and that those tested are recruited to chromatin. While SIR complex assembly and Sir3 self-association are unaffected by the mutations, both classes of mutants, those with mutations in the BAH domain and the L738P mutant, exhibit defective nucleosome or histone binding. BAH mutants lose their association with the nucleosome, whereas Sir3-L738P binds to H4 tail residues 15 to 34 more tightly than wild-type Sir3, an interaction that is independent of the BAH domain. These findings demonstrate that two independent histone-binding activities of Sir3 are required for spreading along chromatin and for gene silencing, and furthermore, identify a surface on the BAH domain that mediates nucleosome binding.

The striking observation that most of the mutations lie in the BAH domain underscores the central role of this domain in silencing. Based on the structural information about the BAH domain, all mutations cluster to a single surface. Interestingly,

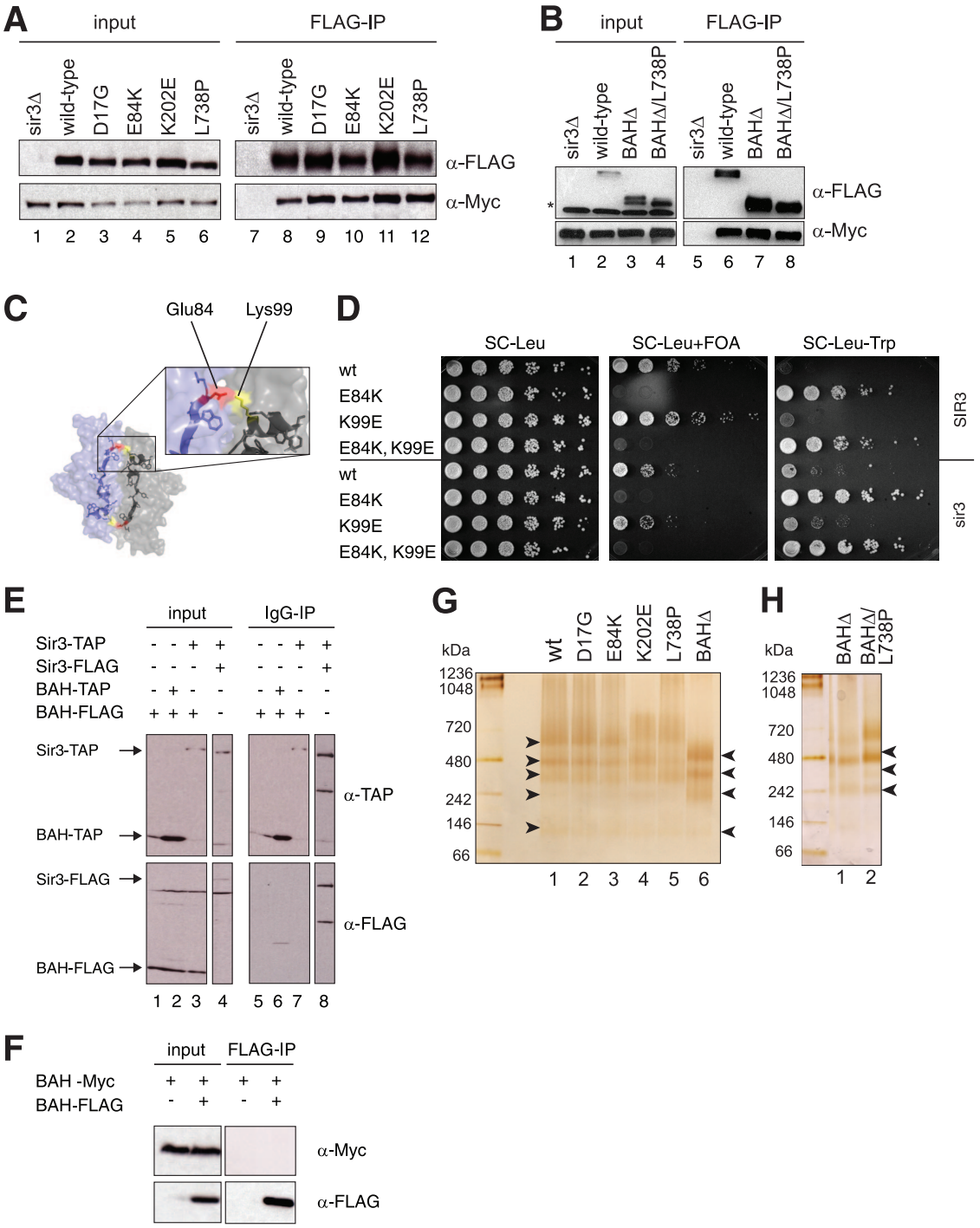

FIG. 7. Sir3 self-interactions are unaffected by point mutations or deletion of the BAH domain. (A) The indicated Sir3-3xFLAG proteins were expressed from a *CEN* plasmid in cells expressing *SIR3-13MYC*$_{13}$. Coimmunoprecipitation for the FLAG tag indicated that none of the mutants disrupted Sir3 dimerization. (B) Coimmunoprecipitation as described for panel A; Sir3-BAHΔ and Sir3-BAHΔ/L738P interact with wild-type Sir3. The asterisk on the left indicates a cross-reacting background band. (C) One of the two BAH-BAH interfaces in the crystal structure described by Connelly et al. (6), highlighting a potential salt bridge. Glu84 is shown in red and Lys99 in yellow. (D) Silencing assays as described in the Fig. 2 (SIR3) and Fig. 3 (sir3Δ) legends. Sir3-K99E does not display a dominant negative silencing defect and Sir3-E84K/K99E does not restore silencing. +FOA, with fluoroorotic acid; −Trp, without tryptophan. (E) The BAH domain does not interact with itself (lane 6) or with full-length Sir3 (lane 7) in coimmunoprecipitation assays. TAP, dual protein A-CBP tag. (F) BAH-3xFLAG does not interact with Sir3-BAHΔ-13xMyc. (G) Sir3 oligomerization is unaffected by point mutations or deletion of the BAH domain. Sir3-3xFLAG was expressed from a high-copy Gal1 vector and purified via the FLAG tag. Three micrograms protein was resolved by native PAGE and silver stained. The pattern of oligomers (identified by arrows) is unchanged by point mutations and is shifted down for the smaller Sir3-BAHΔ protein. (H) As described for panel G but using Sir3-BAHΔ/L738P. The double mutant is able to oligomerize as assayed by native PAGE. α, anti; +, present; −, absent.

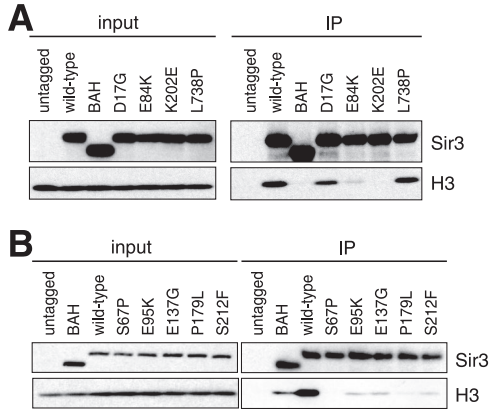

FIG. 8. Loss of nucleosome binding in dominant negative BAH mutants. (A) Results of coimmunoprecipitation assays showing that D17G, E84K, and K202E have decreased binding to nucleosomes. L738P does not interfere with nucleosome binding as shown by the results of this assay. (B) Loss of nucleosome binding in the BAH point mutants S67P, E95K, E137G, P179L, and S212F.

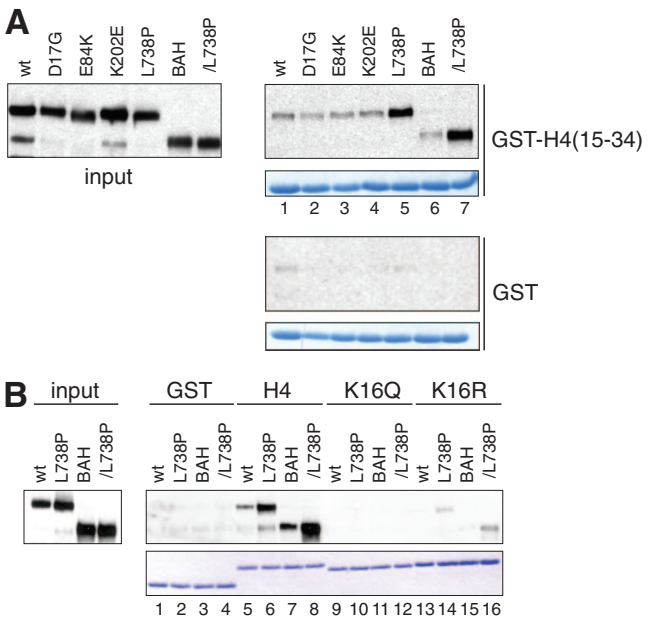

FIG. 9. In vitro histone tail-binding assay. (A) Sir3-L738P binds the histone tail more tightly, both in full-length Sir3 and Sir3-BAHΔ. The BAH domain does not contribute to binding as shown by the results of this assay. GST-H4(15–34) was incubated with Sir3 purified from yeast, and binding was detected by Western blotting. (B) Sir3-L738P binding is sensitive to mutations of residue 16. H4K16Q completely disrupts the interaction, whereas H4K16R binds to Sir3-L738P weakly. wt, wild type.

previously identified mutations that affect silencing are also found on this same surface. Whereas we found that the replacement of Trp86 with glycine is dominant negative for silencing, the replacement of Trp86 with arginine (*SIR3R1*) suppresses a variety of histone H4 N-terminal mutations (21, 22). Similarly, the D205N substitution (*SIR3R3*) suppresses histone tail mutants as well as an allele of *RAP1* that is defective for silencing (21, 22). It is still unclear how these suppressors act, but the D205N mutation has been reported to increase Sir3 binding to DNA and nucleosomes, thus potentially stabilizing Sir3 binding to chromatin through this tightened interaction (6). The L96F mutation was previously isolated from a screen for enhancers of *sir1* (45). While the screening was for a different phenotype, most mutations recovered in that screen were located in the BAH domain as well; consistent with our results, those mutations that are reported to cause a strong dominant telomeric silencing defect are located on the same surface of the BAH domain as the mutations we identified (not shown). Another previously identified mutation in the BAH domain, the temperature-sensitive allele *sir3-8* (E131K) (37, 45), is found in close proximity to all dominant mutations in the primary sequence but is buried on the reverse side of the structure. Interestingly, Glu131 does not dominantly disrupt telomeric silencing (45), which serves as further evidence that only mutations on the nucleosome-binding surface defined in this screen cause this type of defect.

Our screen was not saturated for BAH mutations, as we did not recover most of the BAH mutations previously reported to dominantly disrupt silencing (45). However, for the C-terminal half of Sir3, the screen appears to be saturated, as L738P was isolated repeatedly from two different PCR fragments; it therefore seems unlikely that this form of mutagenesis would have yielded further mutants in this region of Sir3. Based on published AAA^+ domain structures, as well as on secondary structure predictions, Leu738 is expected to lie within an α-helix (7, 33). The fact that no other amino acid substitutions were recovered except for L738P may be due to the disruptive nature of proline within helices, which may create a unique conformation in the AAA^+ domain.

Dominant negative Sir3 mutations and their association with chromatin. Our results indicate that the dominant negative Sir3 mutants directly interfere with silent chromatin formation. All mutants tested are recruited to chromatin, suggesting that they act by directly interfering with silencing, rather than disrupting silent chromatin through other mechanisms, such as by sequestration of essential silencing factors or poisoning the soluble SIR complex and preventing its recruitment to chromatin. Further supporting this idea, BAH mutants expressed as BAH-only truncations do not dominantly disrupt silencing, suggesting that the dominant defect of mutant BAH domains depends on their recruitment to chromatin through the C-terminal domain.

When expressed in the absence of wild-type *SIR3*, the mutants are recruited to the end of the chromosome but do not bind to sites distal to the telomere. This enrichment pattern is identical to Sir3 binding in cells that lack Sir2, in which the SIR complex is unable to spread from silencers (16, 28, 39). The reduced binding of Sir3 at the telomere (*TEL0.07*) in *sir3* mutant and *sir2*Δ cells may be due to the fact that Sir binding at more-distal sites contributes to the stabilization of SIR components at the silencers. In addition, the resolution of ChIP is limited by the fragment shear size of the DNA such that the binding of Sir3 molecules to chromatin more distally would also increase the ChIP signal at the end of the chromosome. We therefore believe that the mutants tested have little or no defect in initial recruitment to chromatin but are defective in

spreading the silencing complex. Similarly to the point mutants, Sir3-BAHΔ binds at *TEL0.07* but fails to spread to *TEL0.7* (34). Therefore, in addition to behaving identically in silencing assays, BAH point mutants and the BAH deletion have an identical spreading defect. Since all BAH mutations we tested cause a similar defect in nucleosome association (Fig. 8), it seems likely that the defect in spreading in BAH point mutants is due to loss of binding to the nucleosome.

Dominant negative Sir3 mutations do not affect the integrity of the SIR complex or Sir3 self-association. Since initial recruitment depends on binding to Sir4, it is unsurprising that the dominant negative Sir3 mutants examined in this study do not disrupt the integrity of the SIR complex. In fact, mutations in Sir4 that disrupt its interaction with Sir3 fail to recruit Sir3 to chromatin (38); by extension, mutations within Sir3 that disrupt this same interaction would most likely fail to be recruited to chromatin, and therefore, would not act as dominant negatives as they can be out-competed by wild-type Sir3.

Surprisingly, none of the dominant negative mutants that we tested disrupt Sir3 self-association as detected in coimmunoprecipitation and native gel assays. It is possible that oligomerization mutants were not identified because only a limited number of all possible substitutions are sampled by PCR-mediated mutagenesis. However, given the sensitivity of the screen and the large number of mutants found, this possibility seems unlikely. Rather, the lack of oligomerization mutants suggests that this type of defect may be recessive.

Based on the crystal structure, it has been suggested that the BAH domain may participate in oligomerization or constitute the major oligomerization domain (6). This seems unlikely for two reasons. First, we were unable to detect an interaction of the BAH domain with itself in vivo. Second, oligomerization in vitro with purified Sir3 is independent of the BAH domain, as Sir3-BAHΔ has the same pattern in the native gel assays as full-length Sir3. Furthermore, we were unable to detect an association of the BAH domain with Sir3-BAHΔ, as would be expected in a head-to-tail arrangement of Sir3 oligomers. It is presently unclear which domain(s) does contribute to oligomerization. The AAA^+ domain is a potential candidate because previously characterized related domains within the same domain subfamily are capable of forming oligomers in an ATP-dependent manner (7, 8). Given the role of AAR in silencing, it remains an attractive hypothesis that AAR replaces ATP in extended Sir3 oligomers, binding between individual subunits of the domain.

Identification of a surface in the BAH domain that mediates Sir3-nucleosome interactions. Based on the finding that two suppressors, W86G and D205N, rescue silencing defects in histone tail mutants (22), we have previously suggested that the surface marked by the suppressors constitutes the main binding surface for histones (34). The finding that the BAH mutations map to the same side of the domain and disrupt the interaction of Sir3 with the nucleosome now provides direct evidence that the Sir3-nucleosome interaction is mediated by this BAH surface. While all mutants tested for nucleosome binding completely disrupt silencing in vivo, some exhibit only a partial defect in nucleosome binding, most notably, D17G. We cannot rule out that D17G has additional defects, given that it is the only residue not located directly on the main interaction surface. However, another mutation that affects the extreme N terminus of Sir3, *ard1*Δ, strongly disrupts Sir3 binding to nucleosomes (34) and has a silencing defect in vivo (46, 51), indicating that this interaction is sensitive to other alterations in the N-terminal β-sheets.

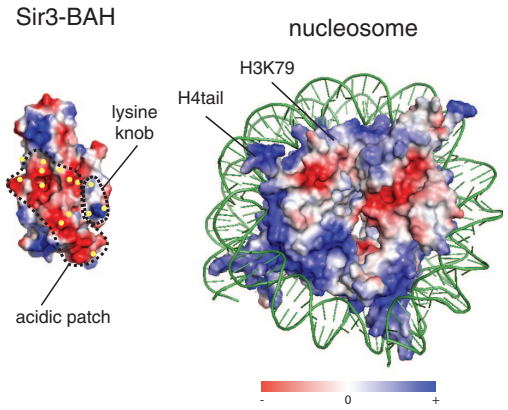

FIG. 10. Electrostatic maps of the BAH domain of Sir3 (PDB-ID 2FL7) (17) and the surface of the yeast nucleosome (PDB-ID 1ID3) (52). The locations of the dominant negative mutations are indicated by yellow dots on BAH. Most of the residues which were mutated lie in an acidic patch, with the exception of the residues mutated as K202E and K209R/K209RG, which constitute a "lysine knob." The histone H4 tail and H3K79 regions on the surface of the nucleosome may constitute an interaction region for the acidic patch in the BAH domain. The lysine knob may interact with DNA or the acidic patch near the H3K79 region on the surface of the nucleosome. See text for details.

As reported by Connelly et al., the surface of the BAH domain is highly negatively charged (Fig. 10) (6). An extensive acidic patch on the dominant negative surface encompasses the majority of mutations identified in our screen. Given the basic nature of the histone H4 N-terminal tail and adjacent regions on the nucleosomal surface (Fig. 10), we propose that this region of the BAH domain directly interacts with the H4 tail/H3 K79 region of the nucleosome. Notably, three residues in this patch, Glu84, Glu95, and Glu137, either lose or reverse their negative charge when mutated. Thus, it seems likely that the mutations within this patch directly disrupt the interaction with this domain of the nucleosome.

In contrast to the majority of residues which were mutated, Lys202 and Lys209 constitute a positively charged "knob" (Fig. 10). Both residues, as well as Lys219, which is not part of the crystal structure, were mutated to glutamate in this screen, reversing their charge. Lys202 and Lys209 also flank Asp205, the residue mutated in *SIR3R3* which increases the affinity of Sir3 for DNA and nucleosomes. Since these lysine residues define a positively charged region, we propose that this area directly interacts with nucleosomal DNA and that their mutation directly interferes with this interaction (Fig. 10). Alternatively, the region adjacent to histone H3 lysine 79 (H3K79) forms a negatively charged surface on the globular domain of the nucleosome (Fig. 10). Sir3 binding to the nucleosome has been shown to be sensitive to the identity and methylation state of H3K79 (1, 34), suggesting that it directly interacts with this region. Therefore, the lysine knob on the BAH domain may plug into this negatively charged patch of the nucleosomal surface.

The observation that mutations in both the acidic patch and

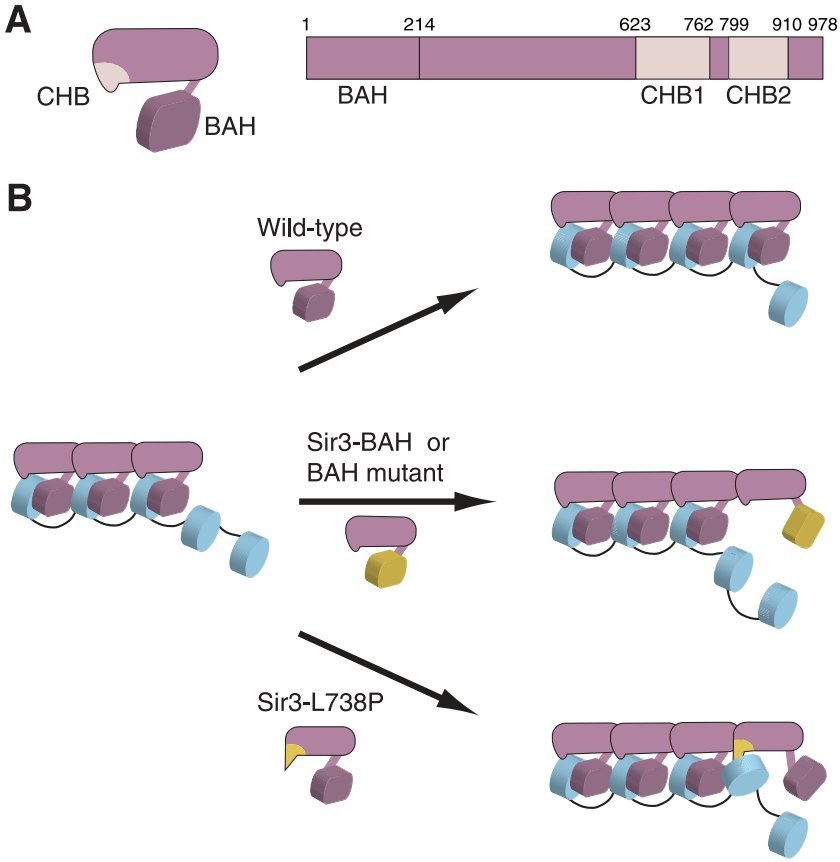

FIG. 11. Model for the role of Sir3 in spreading of silent chromatin. (A) Diagram of Sir3 and its histone/nucleosome-interacting domains. (B) Wild-type Sir3 can be recruited to chromatin through Sir3-Sir3 interactions. Sir3 anchors the spreading SIR complex to chromatin by interactions of CHB and BAH domains with the nucleosome (blue). BAH point mutants or the BAH deletion are unable to bind to the nucleosome, thus resulting in a loss of the anchoring function and of stable recruitment of additional Sir3 molecules. Sir3-L738P may bind to the nucleosome in a conformation that does not allow the BAH domain to engage with the nucleosome on the opposite face.

the positively charged lysine knob disrupt the interaction with nucleosomes supports a model in which multiple individual interactions are required for the stable association of the BAH domain with the nucleosome. Ultimately, structural studies will be needed to determine how the BAH domain binds to the nucleosome.

Increased affinity for the H4 N terminus in Sir3-L738P mutants. Unexpectedly, Sir3-L738P bound to the histone tail region of H4 more strongly than wild-type Sir3. This binding is not caused by nonspecific association of Sir3-L738P with histone tails or GST, since the negative control and a K16Q mutant tail showed no increase in binding and the H4K16R tail strongly reduced binding of Sir3-L738P. While the molecular basis for the increased binding of Sir3-L738P to the H4 tail is still unclear, this finding demonstrates that increased affinity of the SIR complex for histones does not automatically translate to increased silencing in vivo.

In contrast to the results of the coimmunoprecipitation experiments, the binding of Sir3 to GST-histone H4 tail fusions is independent of the BAH domain. The fact that the BAH domain does not contribute to binding in this assay is consistent with the idea that it binds to a patch on the nucleosomal core that also encompasses H3K79. Even though a weak interaction was detected by surface plasmon resonance between BAH and the histone tail of H4 (residues 1 to 34) (34), H4 residues 15 to 34 may constitute too small a surface to stably bind BAH in the peptide binding assay. Given that the BAH domain and the CHB regions of Sir3 compete for the same binding surface, the increased affinity of Sir3-L738P may displace the BAH domain from the nucleosome, thus causing the dominant silencing defect. Alternatively, the tighter interaction of Sir3-L738P may be indicative of a nonproductive conformation which may disrupt spreading through other, downstream effects. A third possible defect caused by the L738P mutation may be nonspecific binding of Sir3-L738P to chromatin, with subsequent sequestering of the SIR complex away from its usual targets. However, this seems unlikely since we did not observe higher levels of Sir3-L738P association with the euchromatic *ACT1* locus.

Model for association of the SIR complex with the nucleosome and its spreading along the chromatin fiber. It has become clear that Sir3 contains multiple histone-binding domains, which seem to bind to partially overlapping regions on the nucleosome and may therefore compete with each other for binding to the nucleosome. The fact that there is overlapping specificity for binding may reflect discrete steps in silent chromatin formation, for example, with an initial interaction by CHB subsequently replaced by a stable BAH-nucleosome as-

sociation. Alternatively, multiple Sir3-nucleosome interactions may occur concurrently and form part of the structure of silent chromatin.

Based on our observations, we propose a model in which the BAH domain binds to one nucleosomal face while the CHB domains bind to the H3 and H4 tails on the opposite face. In this model, the Sir3 protein acts as a tongs-like clamp that grasps the nucleosome, with the BAH and CHB domains acting as two arms that contact opposite surfaces of the nucleosome. During normal spreading (Fig. 11B, top), Sir3 subunits are recruited to chromatin cooperatively through Sir3-Sir3 and Sir3-Sir2/Sir4 interactions (Sir2/Sir4 is not shown in Fig. 11). After this initial recruitment event, the BAH domain interacts with the nucleosome, which must first be deacetylated by Sir2. However, upon recruitment of Sir3 with a mutant BAH domain (Fig. 11B, middle), the mutant BAH domain cannot bind to the deacetylated nucleosome. As a result, the complex is no longer anchored to chromatin, resulting in the disruption of silencing. While Sir3 may still oligomerize, the Sir3 fiber would form independently of chromatin, "derailing" the silencing complex. The incorporation of L738P, which binds the H4K16 region more tightly than wild-type Sir3, may block spreading by promoting an unproductive conformation such that the BAH arm of Sir3 cannot grasp its surface of the nucleosome (Fig. 11B, bottom). This model provides an explanation for the existence of multiple histone-binding domains in the Sir3 protein. Furthermore, our results suggest that the coordination of these binding activities plays a crucial role in the assembly of silent chromatin domains.

ACKNOWLEDGMENTS

We thank Jef Boeke and Rolf Sternglanz for helpful discussions and for sharing results prior to publication and thank Brian Hall for his assistance with the structural analysis and PyMol software. We also thank members of the Moazed laboratory for support and helpful discussions.

This work was supported by a Howard Hughes Medical Institute predoctoral fellowship (J.R.B.), a National Science Foundation predoctoral fellowship (M.O.), and a National Institutes of Health grant (D.M.; RO1-GM061641).

REFERENCES

1. **Altaf, M., R. T. Utley, N. Lacoste, S. Tan, S. D. Briggs, and J. Côté.** 2007. Interplay of chromatin modifiers on a short basic patch of histone H4 tail defines the boundary of telomeric heterochromatin. Mol. Cell **28:**1002–1014.
2. **Ausubel, F. M.** 2002. Short protocols in molecular biology: a compendium of methods from current protocols in molecular biology, 5th ed. Wiley, New York, NY.
3. **Bell, S. P., J. Mitchell, J. Leber, R. Kobayashi, and B. Stillman.** 1995. The multidomain structure of Orc1p reveals similarity to regulators of DNA replication and transcriptional silencing. Cell **83:**563–568.
4. **Buker, S. M., T. Iida, M. Bühler, J. Villén, S. P. Gygi, J. Nakayama, and D. Moazed.** 2007. Two different Argonaute complexes are required for siRNA generation and heterochromatin assembly in fission yeast. Nat. Struct. Mol. Biol. **14:**200–207.
5. **Christianson, T. W., R. S. Sikorski, M. Dante, J. H. Shero, and P. Hieter.** 1992. Multifunctional yeast high-copy-number shuttle vectors. Gene **110:** 119–122.
6. **Connelly, J. J., P. Yuan, H. C. Hsu, Z. Li, R. M. Xu, and R. Sternglanz.** 2006. Structure and function of the *Saccharomyces cerevisiae* Sir3 BAH domain. Mol. Cell. Biol. **26:**3256–3265.
7. **Erzberger, J. P., and J. M. Berger.** 2006. Evolutionary relationships and structural mechanisms of AAA+ proteins. Annu. Rev. Biophys. Biomol. Struct. **35:**93–114.
8. **Erzberger, J. P., M. L. Mott, and J. M. Berger.** 2006. Structural basis for ATP-dependent DnaA assembly and replication-origin remodeling. Nat. Struct. Mol. Biol. **13:**676–683.
9. **Gotta, M., F. Palladino, and S. M. Gasser.** 1998. Functional characterization of the N terminus of Sir3p. Mol. Cell. Biol. **18:**6110–6120.
10. **Gottschling, D. E., O. M. Aparicio, B. L. Billington, and V. A. Zakian.** 1990. Position effect at S. cerevisiae telomeres: reversible repression of Pol II transcription. Cell **63:**751–762.
11. **Grewal, S. I., and D. Moazed.** 2003. Heterochromatin and epigenetic control of gene expression. Science **301:**798–802.
12. **Hartwell, L. H.** 1980. Mutants of Saccharomyces cerevisiae unresponsive to cell division control by polypeptide mating hormone. J. Cell Biol. **85:**811–822.
13. **Hecht, A., T. Laroche, S. Strahl-Bolsinger, S. M. Gasser, and M. Grunstein.** 1995. Histone H3 and H4 N-termini interact with SIR3 and SIR4 proteins: a molecular model for the formation of heterochromatin in yeast. Cell **80:**583–592.
14. **Hecht, A., S. Strahl-Bolsinger, and M. Grunstein.** 1996. Spreading of transcriptional repressor SIR3 from telomeric heterochromatin. Nature **383:**92–96.
15. **Holmes, S. G., A. B. Rose, K. Steuerle, E. Saez, S. Sayegh, Y. M. Lee, and J. R. Broach.** 1997. Hyperactivation of the silencing proteins, Sir2p and Sir3p, causes chromosome loss. Genetics **145:**605–614.
16. **Hoppe, G. J., J. C. Tanny, A. D. Rudner, S. A. Gerber, S. Danaie, S. P. Gygi, and D. Moazed.** 2002. Steps in assembly of silent chromatin in yeast: Sir3-independent binding of a Sir2/Sir4 complex to silencers and role for Sir2-dependent deacetylation. Mol. Cell. Biol. **22:**4167–4180.
17. **Hou, Z., J. R. Danzer, C. A. Fox, and J. L. Keck.** 2006. Structure of the Sir3 protein bromo adjacent homology (BAH) domain from S. cerevisiae at 1.95 A resolution. Protein Sci. **15:**1182–1186.
18. **Huang, J., and D. Moazed.** 2003. Association of the RENT complex with nontranscribed and coding regions of rDNA and a regional requirement for the replication fork block protein Fob1 in rDNA silencing. Genes Dev. **17:**2162–2176.
19. **Imai, S., C. M. Armstrong, M. Kaeberlein, and L. Guarente.** 2000. Transcriptional silencing and longevity protein Sir2 is an NAD-dependent histone deacetylase. Nature **403:**795–800.
20. **Jackson, M. D., and J. M. Denu.** 2002. Structural identification of 2′- and 3′-O-acetyl-ADP-ribose as novel metabolites derived from the Sir2 family of beta-NAD+-dependent histone/protein deacetylases. J. Biol. Chem. **277:** 18535–18544.
21. **Johnson, L. M., G. Fisher-Adams, and M. Grunstein.** 1992. Identification of a non-basic domain in the histone H4 N-terminus required for repression of the yeast silent mating loci. EMBO J. **11:**2201–2209.
22. **Johnson, L. M., P. S. Kayne, E. S. Kahn, and M. Grunstein.** 1990. Genetic evidence for an interaction between SIR3 and histone H4 in the repression of the silent mating loci in Saccharomyces cerevisiae. Proc. Natl. Acad. Sci. USA **87:**6286–6290.
23. **King, D. A., B. E. Hall, M. A. Iwamoto, K. Z. Win, J. F. Chang, and T. Ellenberger.** 2006. Domain structure and protein interactions of the silent information regulator Sir3 revealed by screening a nested deletion library of protein fragments. J. Biol. Chem. **281:**20107–20119.
24. **Landry, J., J. T. Slama, and R. Sternglanz.** 2000. Role of NAD(+) in the deacetylase activity of the SIR2-like proteins. Biochem. Biophys. Res. Commun. **278:**685–690.
25. **Le, S., C. Davis, J. B. Konopka, and R. Sternglanz.** 1997. Two new S-phase-specific genes from Saccharomyces cerevisiae. Yeast **13:**1029–1042.
26. **Liaw, H., and A. J. Lustig.** 2006. Sir3 C-terminal domain involvement in the initiation and spreading of heterochromatin. Mol. Cell. Biol. **26:**7616–7631.
27. **Liou, G. G., J. C. Tanny, R. G. Kruger, T. Walz, and D. Moazed.** 2005. Assembly of the SIR complex and its regulation by O-acetyl-ADP-ribose, a product of NAD-dependent histone deacetylation. Cell **121:**515–527.
28. **Luo, K., M. A. Vega-Palas, and M. Grunstein.** 2002. Rap1-Sir4 binding independent of other Sir, yKu, or histone interactions initiates the assembly of telomeric heterochromatin in yeast. Genes Dev. **16:**1528–1539.
29. **McBryant, S. J., C. Krause, and J. C. Hansen.** 2006. Domain organization and quaternary structure of the Saccharomyces cerevisiae silent information regulator 3 protein, Sir3p. Biochemistry (Moscow) **45:**15941–15948.
30. **Moazed, D.** 2001. Common themes in mechanisms of gene silencing. Mol. Cell **8:**489–498.
31. **Moazed, D., A. Kistler, A. Axelrod, J. Rine, and A. D. Johnson.** 1997. Silent information regulator protein complexes in Saccharomyces cerevisiae: a SIR2/SIR4 complex and evidence for a regulatory domain in SIR4 that inhibits its interaction with SIR3. Proc. Natl. Acad. Sci. USA **94:**2186–2191.
32. **Moretti, P., K. Freeman, L. Coodly, and D. Shore.** 1994. Evidence that a complex of SIR proteins interacts with the silencer and telomere-binding protein RAP1. Genes Dev. **8:**2257–2269.
33. **Neuwald, A. F., L. Aravind, J. L. Spouge, and E. V. Koonin.** 1999. AAA+: a class of chaperone-like ATPases associated with the assembly, operation, and disassembly of protein complexes. Genome Res. **9:**27–43.
34. **Onishi, M., G. G. Liou, J. R. Buchberger, T. Walz, and D. Moazed.** 2007. Role of the conserved Sir3-BAH domain in nucleosome binding and silent chromatin assembly. Mol. Cell **28:**1015–1028.
35. **Renauld, H., O. M. Aparicio, P. D. Zierath, B. L. Billington, S. K. Chhablani, and D. E. Gottschling.** 1993. Silent domains are assembled continuously from the telomere and are defined by promoter distance and strength, and by SIR3 dosage. Genes Dev. **7:**1133–1145.

36. **Richards, E. J., and S. C. Elgin.** 2002. Epigenetic codes for heterochromatin formation and silencing: rounding up the usual suspects. Cell **108:**489–500.
37. **Rine, J., and I. Herskowitz.** 1987. Four genes responsible for a position effect on expression from HML and HMR in Saccharomyces cerevisiae. Genetics **116:**9–22.
38. **Rudner, A. D., B. E. Hall, T. Ellenberger, and D. Moazed.** 2005. A nonhistone protein-protein interaction required for assembly of the SIR complex and silent chromatin. Mol. Cell. Biol. **25:**4514–4528.
39. **Rusché, L. N., A. L. Kirchmaier, and J. Rine.** 2002. Ordered nucleation and spreading of silenced chromatin in Saccharomyces cerevisiae. Mol. Biol. Cell **13:**2207–2222.
40. **Rusché, L. N., A. L. Kirchmaier, and J. Rine.** 2003. The establishment, inheritance, and function of silenced chromatin in Saccharomyces cerevisiae. Annu. Rev. Biochem. **72:**481–516.
41. **Sikorski, R. S., and P. Hieter.** 1989. A system of shuttle vectors and yeast host strains designed for efficient manipulation of DNA in Saccharomyces cerevisiae. Genetics **122:**19–27.
42. **Singer, M. S., and D. E. Gottschling.** 1994. TLC1: template RNA component of Saccharomyces cerevisiae telomerase. Science **266:**404–409.
43. **Smith, J. S., C. B. Brachmann, I. Celic, M. A. Kenna, S. Muhammad, V. J. Starai, J. L. Avalos, J. C. Escalante-Semerena, C. Grubmeyer, C. Wolberger, and J. D. Boeke.** 2000. A phylogenetically conserved NAD+-dependent protein deacetylase activity in the Sir2 protein family. Proc. Natl. Acad. Sci. USA **97:**6658–6663.
44. **Stone, E. M., and L. Pillus.** 1998. Silent chromatin in yeast: an orchestrated medley featuring Sir3p. Bioessays **20:**30–40.
45. **Stone, E. M., C. Reifsnyder, M. McVey, B. Gazo, and L. Pillus.** 2000. Two classes of sir3 mutants enhance the sir1 mutant mating defect and abolish telomeric silencing in Saccharomyces cerevisiae. Genetics **155:**509–522.
46. **Stone, E. M., M. J. Swanson, A. M. Romeo, J. B. Hicks, and R. Sternglanz.** 1991. The *SIR1* gene of *Saccharomyces cerevisiae* and its role as an extragenic suppressor of several mating-defective mutants. Mol. Cell. Biol. **11:**2253–2262.
47. **Suka, N., Y. Suka, A. A. Carmen, J. Wu, and M. Grunstein.** 2001. Highly specific antibodies determine histone acetylation site usage in yeast heterochromatin and euchromatin. Mol. Cell **8:**473–479.
48. **Tanner, K. G., J. Landry, R. Sternglanz, and J. M. Denu.** 2000. Silent information regulator 2 family of NAD-dependent histone/protein deacetylases generates a unique product, 1-O-acetyl-ADP-ribose. Proc. Natl. Acad. Sci. USA **97:**14178–14182.
49. **Tanny, J. C., G. J. Dowd, J. Huang, H. Hilz, and D. Moazed.** 1999. An enzymatic activity in the yeast Sir2 protein that is essential for gene silencing. Cell **99:**735–745.
50. **Tanny, J. C., and D. Moazed.** 2001. Coupling of histone deacetylation to NAD breakdown by the yeast silencing protein Sir2: evidence for acetyl transfer from substrate to an NAD breakdown product. Proc. Natl. Acad. Sci. USA **98:**415–420.
51. **Wang, X., J. J. Connelly, C. L. Wang, and R. Sternglanz.** 2004. Importance of the Sir3 N terminus and its acetylation for yeast transcriptional silencing. Genetics **168:**547–551.
52. **White, C. L., R. K. Suto, and K. Luger.** 2001. Structure of the yeast nucleosome core particle reveals fundamental changes in internucleosome interactions. EMBO J. **20:**5207–5218.
53. **Zhang, Z., M. K. Hayashi, O. Merkel, B. Stillman, and R. M. Xu.** 2002. Structure and function of the BAH-containing domain of Orc1p in epigenetic silencing. EMBO J. **21:**4600–4611.
54. **Zheng, L., U. Baumann, and J. L. Reymond.** 2004. An efficient one-step site-directed and site-saturation mutagenesis protocol. Nucleic Acids Res. **32:**e115.